CAPACITY ANALYSIS OF WCC-FBMC/OQAM SYSTEMS

Màrius Caus[⋆] *Ana I. Perez-Neira*[⋆†] *Adrian Kliks*[‡] *Quentin Bodinier*[∗] *Faouzi Bader*[∗]

[⋆] CTTC, Castelldefels, Barcelona, Spain
[†]Dept. of Signal Theory and Communications, UPC, Barcelona, Spain
[‡]Chair of Wireless Communications, PUT, Poznan, Poland
[∗]SCEE/IETR CentraleSupélec, Rennes, France

ABSTRACT

This paper evaluates the capacity of weighted circularly convolved FBMC/OQAM systems. A rigorous mathematical model is derived to calculate the increase of capacity that can be obtained thanks to the lattice structure of the modulation and the exploitation of the intrinsic interference. The numerical results reveal that a signal to noise ratio gain of 2dB is obtained in one resource block of 12 subcarriers, translating into a capacity increase of 11% with respect to OFDM, which nuances some previous results on this topic in the literature.

1. INTRODUCTION

Orthogonal frequency division multiplexing (OFDM), though spectrally agile and easily implementable, has a poor stopband attenuation and suffers from a spectral efficiency degradation, due to the cyclic prefix (CP) transmission [1]. One alternative to OFDM is the filter bank multicarrier modulation in conjunction with offset QAM (FBMC/OQAM), because no CP is needed and subcarrier signals exhibit good time-frequency localization (TFL) properties [2, 3]. Although FBMC/OQAM can theoretically achieve the maximum Nyquist rate, the tails of the pulses yield an overhead in burst transmission. This disadvantage is counteracted to some extent by adopting the circular convolution. This scheme, which is referred to as weighted circularly convolved FBMC/OQAM (WCC-FBMC/OQAM) [4], preserves the real-domain orthogonality. Therefore, WCC-FBMC/OQAM is characterized by the presence of an intrinsic interference.

It is worth mentioning that sometimes the interference can be exploited, for instance, to improve the estimation of the channel [5]. Bearing this result in mind, this paper aims to precisely answer the question: how much can the capacity of WCC-FBMC/OQAM be increased with respect to OFDM? It has been shown in [6] that a signal to noise ratio (SNR) gain of approximately 3dB can be expected on each subcarrier, by treating the interference as useful information. Then, it becomes evident that the complete utilization of the interference improves the capacity. Nevertheless, the method addressed in [6] takes from granted that interference terms received on different frequency-time (FT) positions are independent, which is not the case in neither FBMC/OQAM nor WCC-FBMC/OQAM. In order to conduct a thorough and rigorous capacity analysis, we derive an analytical model that takes into account: (i) the correlation of the interference, (ii) the improperness nature of the symbols, (iii) the lattice structure and (iv) the overhead in burst transmission. The proposed method reveals that the information extracted from the interference yields a maximum SNR gain of 2 dB in one resource block (RB) of 12 subcarriers, which brings a capacity increase of 11% with respect to OFDM.

The remaining of this paper is organized as follows: Section 2 presents the system model. Next, the analysis of the capacity is conducted in Section 3. Finally, Section 4 presents the numerical results and Section 5 draws the conclusions.

2. SYSTEM MODEL

Let us consider a frame-based FBMC/OQAM system with M occupied subcarriers, where the time domain is divided into blocks of N symbols. We assume that no overlapping is observed in neither time nor frequency domains with neighboring blocks. To confine the energy, the transmitted symbols are shaped with time and frequency shifted versions of a low-pass band filter $p[n]$ of length L. In this sense, the subband pulse applied on the mth subcarrier is given by

$$f_m[n] = p[n]e^{j\frac{2\pi}{M}m\left(n-\frac{L-1}{2}\right)}, \ 0 \leq n \leq L-1. \quad (1)$$

At the receive side, the demodulated signal on the qth subcarrier and kth time instant is expressed as [7]:

$$y_q[k] = \sum_{m=M_1}^{M_2} g_{qm}[k] \star (\theta_m[k]d_m[k]) + w_q[k], \quad (2)$$

This work has received funding from the Spanish Ministry of Economy and Competitiveness under projects TEC2014-59255-C3-1-R and Red ARCO 5G, TEC2014-56469-REDT and from the Catalan Government under grant 2014SGR1567. This work was also supported by the European Commission in the framework of the FP7 Network of Excellence in Wireless COMmunications NEWCOM# (Grant agreement no. 318306).

for $0 \leq M_1 \leq q \leq M_2 \leq M-1$ and $0 \leq k \leq N-1$. The number of active subcarriers is $M_a = M_2 - M_1 + 1$ and

$$g_{qm}[k] = \left(f_q^*[-n] \star h[n] \star f_m[n]\right)_{\downarrow \frac{M}{2}} \tag{3}$$

represents the impulse response between the *m*th and the *q*th subchannel, which includes not only the channel impulse response $h[n]$ but also the transmit and reception pulse shapes. The operation $(.)_{\downarrow x}$ downsamples a sequence by a factor of x. Unlike the model presented in [7], we have considered that inter-carrier interference does not exclusively come from the adjacent subcarriers, but may come from more distant ones. The equivalent channel $g_{qm}[k]$ is different from zero for $-L_1 = -\left\lfloor \frac{L-1}{M/2} \right\rfloor \leq k \leq \left\lfloor \frac{L-1+L_{ch}}{M/2} \right\rfloor = L_2$, where L_{ch} denotes the maximum channel excess delay. The function $\lfloor x \rfloor$ gives the largest integer equal or lower than x. The noise at the FT position (q,k) depends on the the noise at the input of the receiver, i.e. $w[n]$, and the matched filter as follows:

$$w_q[k] = \left(f_q^*[-n] \star w[n]\right)_{\downarrow \frac{M}{2}}. \tag{4}$$

It must be noticed that in (2) the symbols $\{d_q[k]\}$, which are drawn from a pulse amplitude modulation (PAM) constellation, are multiplied by this phase term

$$\theta_m[k] = \begin{cases} 1 & k+m \text{ even} \\ j & k+m \text{ odd,} \end{cases} \tag{5}$$

to guarantee that adjacent symbols in the FT plane differ by a phase factor of $\frac{\pi}{2}$. In the remaining of the paper, we consider the case of low time-frequency selective channels, so that the fading can be considered flat within the range of one subcarrier and the whole duration of the frame. Then, the channel seen by the signal transmitted on the *m*th subcarrier is given by H_m, which denotes the frequency response evaluated on the radial frequency $\frac{2\pi m}{M}$, yielding this simplified channel model $g_{qm}[k] = H_m \alpha_{qm}[k]$ [8]. The variable $\alpha_{qm}[k]$ is used to represent the FBMC/OQAM transmultiplexer response, which is given by

$$\begin{aligned} \alpha_{qm}[\tau] \quad &= \left(f_q^*[-n] \star f_m[n]\right)_{\downarrow \frac{M}{2}} = \sum_n (-1)^{\tau q} p[n] \\ &\times p\left[n - \tau \tfrac{M}{2}\right] e^{-j\frac{2\pi}{M}(q-m)\left(n - \frac{L-1}{2}\right)}. \end{aligned} \tag{6}$$

With the aim of clearly highlighting that the demodulated signals are not independent, we propose to stack the samples column-wise. Then, $\mathbf{y}[k] = [y_{M_1}[k] \cdots y_{M_2}[k]]^T$ can be expressed with this matrix notation

$$\mathbf{y}[k] = \sum_{\tau=-L_1}^{L_2} \mathbf{G}[\tau]\mathbf{x}[k-\tau] + \mathbf{w}[k], \quad 0 \leq k \leq N-1, \tag{7}$$

$$\mathbf{x}[k] = [\theta_{M_1}[k] d_{M_1}[k] \cdots \theta_{M_2}[k] d_{M_2}[k]]^T \tag{8}$$

$$\mathbf{w}[k] = [w_{M_1}[k] \cdots w_{M_2}[k]]^T. \tag{9}$$

The matrix $\mathbf{G}[\tau] \in \mathbb{C}^{M_a \times M_a}$ reads

$$\mathbf{G}[\tau] = \mathbf{A}[\tau]\mathbf{H} = \begin{bmatrix} \alpha_{M_1 M_1}[\tau] & \cdots & \alpha_{M_1 M_2}[\tau] \\ \vdots & \ddots & \vdots \\ \alpha_{M_2 M_1}[\tau] & \cdots & \alpha_{M_2 M_2}[\tau] \end{bmatrix} \begin{bmatrix} H_{M_1} & & \\ & \ddots & \\ & & H_{M_2} \end{bmatrix}. \tag{10}$$

Note that $\mathbf{H}$ is diagonal and $\mathbf{A}[\tau]$ only depends on the pulses.

2.1. From FBMC/OQAM to WCC-FBMC/OQAM

It is important to highlight that in FBMC/OQAM systems there is an overhead ratio equal to $\frac{2L-M}{NM}$, because of the tails of the pulse. By replacing the linear convolution with the circular one, the overhead is removed and the length of the burst is reduced from $L + (N-1)M/2$ to $NM/2$ samples, [4]. Sticking to the scenario where the channel frequency response is flat at the subcarrier level, the output of the demodulator is given by

$$\mathbf{y}[k] = \sum_{\tau=-L_1}^{L_2} \mathbf{A}[\tau]\mathbf{H}\mathbf{x}_N[k-\tau] + \mathbf{w}_{cc}[k], \tag{11}$$

when the circular convolution is employed. The sequence $\mathbf{x}_N[k]$ is a periodic extension of $\mathbf{x}[k]$ that reads

$$\mathbf{x}_N[k] = \sum_{i=-\infty}^{\infty} \mathbf{x}[k - Ni]. \tag{12}$$

The summation in (12) corresponds to the case where N is a multiple of four. The rest of the cases have not been covered, but they can be derived by including a weighting coefficient [4]. It appears from (11) that the model is very similar to the one used in FBMC/OQAM, except for the filtered noise, which we now denote by $\mathbf{w}_{cc}[k] = \left[w_{M_1}^{cc}[k] \cdots w_{M_2}^{cc}[k]\right]^T$. The filtered noise in the FT position (q,k) is given by $w_q^{cc}[k]$. Due to the copy-and-append operation performed at the receive side [4], the correlation between $\mathbf{w}_q^{cc} = \left[w_q^{cc}[0] \cdots w_q^{cc}[N-1]\right]^T$ and $\mathbf{w}_m^{cc} = [w_m^{cc}[0] \cdots w_m^{cc}[N-1]]^T$ results in this $N \times N$ circulant matrix

$$\mathbf{R}_{qm} = \mathbb{E}\left\{\mathbf{w}_q^{cc} \left(\mathbf{w}_m^{cc}\right)^H\right\}, \tag{13}$$

with $[r_{qm}[0] ... r_{qm}[-L_1] \ 0 ... 0 \ r_{qm}[L_2] ... r_{qm}[1]]$ in the first row. It is worth highlighting that $\mathbf{R}_{qm}$ can be written as function of the noise correlation in the linear model, i.e. $r_{qm}[k-l] = \mathbb{E}\{w_q[k] w_m^*[l]\}$. The matrix $\mathbf{R}_{qm}$ has been characterized, because it is definitely relevant for the capacity analysis.

3. CAPACITY ANALYSIS

This section evaluates the capacity building upon the model (11). In order to work with easy-to-handle expressions, the analysis will be conducted in the frequency domain. Keeping

in mind that the circular convolution converts to a pointwise product of two N-point discrete Fourier transform (DFT) sequences, the input/output relation at frequency $\frac{2\pi}{N}i$ becomes

$$\mathbf{y}_i = \sum_{k=0}^{N-1} \mathbf{y}[k]e^{-j\frac{2\pi}{N}ik} = \mathbf{G}_i\mathbf{x}_i + \mathbf{w}_i, \;\; i = 0, ..., N-1. \quad (14)$$

Mathematically, $\mathbf{G}_i$, $\mathbf{w}_i$ and $\mathbf{x}_i$ can be respectively written as $\mathbf{G}_i = \sum_{k=-L_1}^{L_2} \mathbf{G}[k]e^{-j\frac{2\pi}{N}ik}$, $\mathbf{w}_i = \sum_{k=0}^{N-1} \mathbf{w}_{cc}[k]e^{-j\frac{2\pi}{N}ik}$ and $\mathbf{x}_i = \sum_{k=0}^{N-1} \mathbf{x}[k]e^{-j\frac{2\pi}{N}ik}$.

It has been assumed that symbols are independent and identically distributed with mean energy symbol $\frac{E_S}{2}$, i.e. $\mathbb{E}\left(d_q[k]d_m[l]\right) = \frac{E_S}{2}\delta_{q,m}\delta_{k,l}$. The factor 2 indicates that the symbols $\{d_q[k]\}$ correspond to either real or imaginary parts of complex-valued QAM symbols, which mean energy is E_S. Before evaluating the capacity it is important to remark that symbols are improper, because the pseudo-covariance matrix does not vanish. In other words, $\mathbb{E}\left\{\mathbf{x}[k]\mathbf{x}^T[k]\right\} \neq \mathbf{0}$. Bearing this assumption in mind, it can be verified that improperness holds true in the frequency domain as well. To deal with the improper nature of the symbols, so that all the second order statistics come into play, we proceed with the definition of these augmented vectors: $\bar{\mathbf{y}}_i = \left[\mathbf{y}_i^T \mathbf{y}_i^H\right]^T$ and $\bar{\mathbf{w}}_i = \left[\mathbf{w}_i^T \mathbf{w}_i^H\right]^T$. Then, the achievable rate under the assumption of improper Gaussian signaling at frequency $\frac{2\pi}{N}i$ can be formulated as (see (10) in [9]):

$$R\left(\frac{2\pi}{N}i\right) = \frac{1}{2}\log_2\frac{\left|\mathbf{C}_{\bar{\mathbf{y}}_i}\right|}{\left|\mathbf{C}_{\bar{\mathbf{w}}_i}\right|}, \quad (15)$$

with $\mathbf{C}_{\bar{\mathbf{y}}_i} = \mathbb{E}\left\{\bar{\mathbf{y}}_i\bar{\mathbf{y}}_i^H\right\}$ and $\mathbf{C}_{\bar{\mathbf{w}}_i} = \mathbb{E}\left\{\bar{\mathbf{w}}_i\bar{\mathbf{w}}_i^H\right\}$. The determinant of a square matrix $\mathbf{S}$ is $|\mathbf{S}|$. The augmented covariance matrices can be partitioned into four blocks as follows:

$$\mathbf{C}_{\bar{\mathbf{y}}_i} = \begin{bmatrix} \mathbf{C}_{\mathbf{y}_i} & \tilde{\mathbf{C}}_{\mathbf{y}_i} \\ \tilde{\mathbf{C}}_{\mathbf{y}_i}^* & \mathbf{C}_{\mathbf{y}_i}^* \end{bmatrix} \quad (16)$$

$$\mathbf{C}_{\bar{\mathbf{w}}_i} = \begin{bmatrix} \mathbf{C}_{\mathbf{w}_i} & \tilde{\mathbf{C}}_{\mathbf{w}_i} \\ \tilde{\mathbf{C}}_{\mathbf{w}_i}^* & \mathbf{C}_{\mathbf{w}_i}^* \end{bmatrix}. \quad (17)$$

After several derivation steps, the authors in [9] have demonstrated that (15) can be compactly expressed in this form

$$R\left(\frac{2\pi}{N}i\right) = \log_2\left|\mathbf{C}_{\mathbf{w}_i}^{-1}\mathbf{C}_{\mathbf{y}_i}\right| + \frac{1}{2}\log_2\frac{\left|\mathbf{I}_{M_a} - \mathbf{C}_{\mathbf{y}_i}^{-1}\tilde{\mathbf{C}}_{\mathbf{y}_i}\mathbf{C}_{\mathbf{y}_i}^{-T}\tilde{\mathbf{C}}_{\mathbf{y}_i}^H\right|}{\left|\mathbf{I}_{M_a} - \mathbf{C}_{\mathbf{w}_i}^{-1}\tilde{\mathbf{C}}_{\mathbf{w}_i}\mathbf{C}_{\mathbf{w}_i}^{-T}\tilde{\mathbf{C}}_{\mathbf{w}_i}^H\right|}. \quad (18)$$

The matrix $\mathbf{I}_{M_a}$ designates the M_a-dimensional identity matrix. It is worth highlighting that the second term in the right-hand side of (18) is equal to zero with proper Gaussian signaling. To evaluate $R\left(\frac{2\pi}{N}i\right)$, it is deemed necessary to characterize the second order moments of the symbols and the noise. To this end, the statistical information of the variables that come into play has been provided in the following sections.

3.1. Statistical information of symbols

Taking into account the statistical information of $\mathbf{x}[k]$, the covariance and the pseudo-covariance matrices of $\mathbf{x}_i$ become

$$\mathbf{C}_{\mathbf{x}_i} = \mathbb{E}\left\{\mathbf{x}_i\mathbf{x}_i^H\right\} = N\frac{E_S}{2}\mathbf{I}_{M_a} \quad (19)$$

$$\tilde{\mathbf{C}}_{\mathbf{x}_i} = \mathbb{E}\left\{\mathbf{x}_i\mathbf{x}_i^T\right\} = \text{diag}\left\{\sum_{k=0}^{N-1}\frac{E_S}{2}\theta_{M_1}^2[k]e^{-2j\frac{2\pi}{N}ik}, \cdots, \sum_{k=0}^{N-1}\frac{E_S}{2}\theta_{M_2}^2[k]e^{-2j\frac{2\pi}{N}ik}\right\}. \quad (20)$$

Due to the fact that real and imaginary parts are interleaved according to (5), the entries of $\tilde{\mathbf{C}}_{\mathbf{x}_i}$ in the (lth,lth) position are

$$\left[\tilde{\mathbf{C}}_{\mathbf{x}_i}\right]_{ll} = (-1)^{M_1+l}\frac{E_S}{2}\sum_{k=0}^{N-1}e^{-j\pi k}e^{-2j\frac{2\pi}{N}ik}, \quad (21)$$

for $0 \leq l \leq M_a - 1$. To simplify the notation it is useful to realize that (21) can be regarded as a truncated geometric series in $e^{-j\left(2\frac{2\pi}{N}i+\pi\right)}$. Then, we end up with

$$\left[\tilde{\mathbf{C}}_{\mathbf{x}_i}\right]_{ll} = (-1)^{M_1+l}\frac{E_S}{2}e^{-j\left(\frac{2\pi}{N}i+\frac{\pi}{2}\right)(N-1)}\frac{\sin\left(\left(\frac{2\pi}{N}i+\frac{\pi}{2}\right)N\right)}{\sin\left(\frac{2\pi}{N}i+\frac{\pi}{2}\right)}. \quad (22)$$

3.2. Statistical information of noise

If the noise samples at the input of the receiver are Gaussian distributed, i.e. $w[n] \sim \mathcal{CN}(0, N_0)$, then the expectation of the filtered noise in the linear model satisfies:

$$\begin{aligned}&\mathbb{E}\left\{\Re\left(w_q[k]\right)\Re\left(w_m[l]\right)\right\} = \\ &\mathbb{E}\left\{\Im\left(w_q[k]\right)\Im\left(w_m[l]\right)\right\} = \frac{N_0}{2}\Re\left(\alpha_{qm}[k-l]\right)\end{aligned} \quad (23)$$

$$\begin{aligned}&-\mathbb{E}\left\{\Re\left(w_q[k]\right)\Im\left(w_m[l]\right)\right\} = \\ &\mathbb{E}\left\{\Im\left(w_q[k]\right)\Re\left(w_m[l]\right)\right\} = \frac{N_0}{2}\Im\left(\alpha_{qm}[k-l]\right).\end{aligned} \quad (24)$$

As a consequence, $\mathbb{E}\left\{w_q[k]w_m[l]\right\} = 0$ and $r_{qm}[k-l] = \mathbb{E}\left\{w_q[k]w_m^*[l]\right\} = N_0\alpha_{qm}[k-l]$. Therefore, $\tilde{\mathbf{C}}_{\mathbf{w}_i} = \mathbf{0}$ and the (pth,lth) position of $\mathbf{C}_{\mathbf{w}_i}$ is defined as

$$\left[\mathbf{C}_{\mathbf{w}_i}\right]_{pl} = \mathbf{f}_N^i\mathbf{R}_{p+M_1l+M_1}\left(\mathbf{f}_N^i\right)^H, \;\; 0 \leq p, l \leq M_a - 1. \quad (25)$$

The row vector $\mathbf{f}_N^i \in \mathbb{C}^{1\times N}$ accounts for the ith row of the N-point DFT matrix. Recalling from (13) that $\mathbf{R}_{p+M_1l+M_1}$ is circulant, it follows that $\mathbf{R}_{p+M_1l+M_1}$ can be factorized with the DFT matrix. Therefore, (25) can be expressed as function of the Fourier transform of $\alpha_{p+M_1l+M_1}[k]$. From the expressions derived in this section, it can be inferred that

$$\left[\mathbf{C}_{\mathbf{w}_i}\right]_{pl} = N \times N_0\sum_{k=-L_1}^{L_2}\alpha_{p+M_1l+M_1}[k]e^{-j\frac{2\pi}{N}ik}. \quad (26)$$

3.3. Capacity in WCC-FBMC/OQAM and OFDM

The capacity can be computed as the integration of supportable information rates over the entire band [10], namely

$$C = \frac{1}{2\pi}\int_0^{2\pi} R(\omega)d\omega. \quad (27)$$

An approximate solution of the capacity can be obtained when the frequency response of the rate does not present strong variation in the range of $\frac{2\pi}{N}$. Then, the capacity in the WCC-FBMC/OQAM context can be simplified as

$$C_{FBMC} \approx 2\frac{NM \times 0.5}{NM \times 0.5 + T_w}\frac{1}{N}\sum_{i=0}^{N-1} R\left(\frac{2\pi}{N}i\right). \quad (28)$$

The higher is N, the closer is the approximation to the exact expression. The ratio $\frac{NM\times 0.5}{NM\times 0.5+Tw}$ characterizes the capacity penalty due to time-windowing, which is of paramount importance to combat the detrimental effects caused by the circular convolution. A windowing length equal to $T_w = M/2$ suffices to significantly improve the side lobe attenuation [4]. Finally, the factor 2 is included to indicate that two FBMC/OQAM multicarrier symbols are transmitted in one OFDM symbol period. With this modification a fair comparison can be performed with OFDM.

If we project the generic case to OFDM systems, it can be verified that the maximum achievable rate is defined as

$$C_{OFDM} = \frac{1}{1+\frac{L_{CP}}{M}}\log_2\left|\mathbf{I}_{M_a} + \frac{(E_S/N_0)}{1+\frac{L_{CP}}{M}}\mathbf{H}\mathbf{H}^H\right|. \quad (29)$$

The spectral efficiency degradation and the waste of energy depend on L_{CP}, which denotes the CP length.

4. RESULTS

This section evaluates the capacity expressions derived in Section 3 for different SNR values, which are defined as $SNR = \frac{E_S}{N_0}$. Parameters are chosen coherently with long term evolution (LTE) specifications in the following way: sampling frequency is set to 15.36 MHz, $M = 1024$, $M_a = 12$, $N = 14$ for OFDM and $N = 28$ for WCC-FBMC/OQAM. It has been experimentally verified that increasing the number of points beyond $N = 28$ does not bring substantial improvements in terms of accuracy. WCC-FBMC/OQAM capacity is computed for both isotropic orthogonal transform algorithm (IOTA) [11] and Bellanger [12] filters with an overlapping factor equal to 4, thus $L = 4M$. The multipath fading has been modeled according to the Extented Pedestrian A (EPA) channel [13], for which (11) can be assumed as the true expression.

The capacity represented in Figure 1.a, which has been divided by M_a, indicates that WCC-FBMC/OQAM outperforms OFDM in 2 dB, from 15 dB to 20 dB. Figure 1.b shows that IOTA-based WCC-FBMC/OQAM systems are able to offer 9-11 % more bits than OFDM in one RB. By resorting to the Bellanger pulse, the increase is around 8%. With $L_{CP} = M/14$ and $T_w = M/2$, we can resolve that $\frac{NM\times 0.5+T_w}{NM\times 0.5}\frac{M}{M+L_{CP}} = 0.9667$. Therefore, the capacity increase that corresponds to the exploitation of the interference is given by $0.9667 \times C_{FBMC}/C_{OFDM}$.

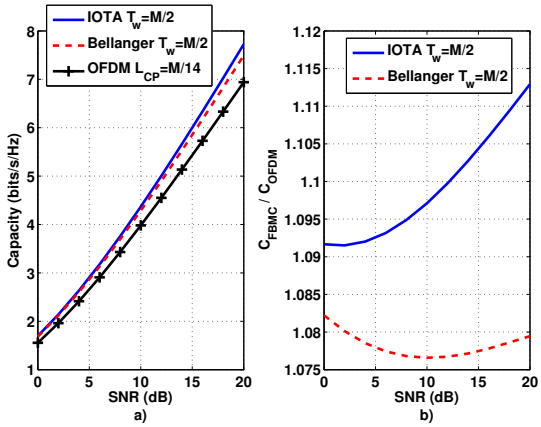

Fig. 1. a) Capacity of OFDM and WCC-FBMC/OQAM systems against SNR. b) Ratio between WCC-FBMC/OQAM and OFDM capacities against SNR.

Better results than those presented in Figure 1 are obtained using the capacity formula for parallel channels [6], yet the interference correlation is not accounted for.

Leveraging on the use of pulse shaping techniques, the capacity can be further increased with respect to OFDM, by reducing the number of subcarriers that remain silent. The case analyzed in [14] allows FBMC/OQAM to achieve an increase of 10% in the capacity. Based on this observation, we shall consider the improvement that stems from the additional occupied subcarriers, which depends on the spectral mask of each scenario, on top of the gain brought by Figure 1.b.

5. CONCLUSION

In this paper we have presented a generic model for WCC-FBMC/OQAM systems, which can be easily tailored to different waveforms. Building upon this model, a thorough analysis of the capacity has been conducted, taking into consideration all the characteristics of the modulation. The numerical results reveal that WCC-FBMC/OQAM outperforms OFDM in 2dB, through the exploitation of intrinsic interference and the lattice structure. It is shown that this gain translates into an increase of 11% in capacity. The increase is more modest than that obtained in other works, because the impact of the interference correlation has not been neglected. Future work should focus on how to practically exploit the intrinsic interference inherent to WCC-FBMC/OQAM systems, in order to perform closer to the capacity.

6. REFERENCES

[1] B. Farhang-Boroujeny, "OFDM versus filter bank multicarrier," *IEEE Signal Process. Mag.*, vol. 28, no. 3, pp. 92–112, May 2011.

[2] P. Siohan, C. Siclet, and N. Lacaille, "Analysis and design of OFDM/OQAM systems based on filterbank theory," *IEEE Trans. Signal Process.*, vol. 50, no. 5, pp. 1170–1183, May 2002.

[3] M. Schellmann, Z. Zhao, H. Lin, P. Siohan, N. Rajatheva, V. Luecken, and A. Ishaque, "FBMC-based air interface for 5G mobile: Challenges and proposed solutions," in *2014 9th International Conference on Cognitive Radio Oriented Wireless Networks and Communications (CROWNCOM)*, 2014, pp. 102–107.

[4] M. J. Abdoli, M. Jia, and J. Ma, "Weighted circularly convolved filtering in OFDM/OQAM," in *Personal Indoor and Mobile Radio Communications (PIMRC), 2013 IEEE 24th International Symposium on*, Sept 2013, pp. 657–661.

[5] C. Lele, P. Siohan, and R. Legouable, "2 dB Better Than CP-OFDM with OFDM/OQAM for Preamble-Based Channel Estimation," in *IEEE International Conference on Communications*, 2008, pp. 1302–1306.

[6] R. Razavi, P. Xiao, and R. Tafazolli, "Information Theoretic Analysis of OFDM/OQAM with Utilized Intrinsic Interference," *IEEE Signal Processing Letters*, vol. 22, no. 5, pp. 618–622, May 2015.

[7] M. Caus, A. Perez Neira, and M. Renfors, "Low-complexity interference variance estimation methods for coded multicarrier systems: application to SFN," *EURASIP Journal on Advances in Signal Processing*, vol. 2013, no. 1, 2013.

[8] C. Lele, J.-P. Javaudin, R. Legouable, A. Skrzypczak, and P. Siohan, "Channel estimation methods for preamble-based OFDM/OQAM modulations," *European Transactions on Telecommunications*, vol. 19, no. 7, pp. 741–750, 2008.

[9] Y. Zeng, C. Yetis, E. Gunawan, Y. L. Guan, and R. Zhang, "Transmit Optimization With Improper Gaussian Signaling for Interference Channels," *IEEE Transactions on Signal Processing*, vol. 61, no. 11, pp. 2899–2913, June 2013.

[10] X. Zhang and S.-Y. Kung, "Capacity analysis for parallel and sequential MIMO equalizers," *IEEE Transactions on Signal Processing*, vol. 51, no. 11, pp. 2989–3002, Nov 2003.

[11] P. Siohan and C. Roche, "Cosine-modulated filterbanks based on extended gaussian functions," *IEEE Transactions on Signal Processing*, vol. 48, no. 11, pp. 3052–3061, 2000.

[12] M. Bellanger, "Specification and design of a prototype filter for filter bank based multicarrier transmission." ICASSP, 2001, pp. 2417–2420.

[13] "3rd Generation Partnership Project; Technical Specification Group Radio Access Network; Evolved Universal Terrestrial Radio Access (E-UTRA); User Equipment (UE) radio transmission and reception; (Release 8)." 3GPP TR 36.803 v1.1.0.

[14] L. Baltar, D. Waldhauser, and J. Nossek, "Out-Of-Band Radiation in Multicarrier Systems: A Comparison," in *Multi-Carrier Spread Spectrum 2007*, ser. Lecture Notes Electrical Engineering. Springer Netherlands, 2007, vol. 1, pp. 107–116.